Study and development of morphological analysis guidelines for point cloud management: The “decisional cube”

STUDY AND DEVELOPMENT OF MORPHOLOGICAL ANALYSIS GUIDELINES FOR POINT CLOUD MANAGEMENT: THE "DECISIONAL CUBE"

Enrico Vezzetti

Dipartimento di Sistemi di Produzione ed Economia dell'Azienda
Politecnico di Torino

Abstract

When talking about reverse engineering, it is necessary to focus on the management of point clouds. Generally speaking, every 3D scanner device codifies simple and complex geometries providing different point cloud densities as an output. Point cloud density is usually more correlated with the technical specifications of the device employed rather than with the morphology of the object acquired. This situation is due to the frequent use of structured grids by a large quantity of devices. In order to solve this problem, we therefore need to integrate the classical structured grid acquisition with a smart selective one, which is able to identify different point cloud densities in accordance with the morphological complexity of the object regions acquired.

Currently, we can reach the destination in many different ways. Each of them is able to provide different performances depending on the object morphology and the performances of 3D scanner devices. Unfortunately, there does not yet exist one universal approach able to be employed in all cases. For this reason, the present paper aims to propose a first analysis of the available methodologies and parameters, in order to provide final users with some guidelines for supporting their decisions according to the specific application they are facing. Moreover, the developed guidelines have been illustrated and validated by a series of case studies of the proposed method.

Keywords: Reverse Engineering, 3D Scanner, Point Cloud Management, Morphological Analysis

1.0 Introduction

Reverse engineering process starts from the usage of a scanning device that usually provides a "point cloud", representing a particular set of points describing a discrete sample of a physical model surface. The Delaunay's approach is only a triangulation technique which can be used to generate a polyhedral model of a physical one, starting from a point cloud. These are only two of the many steps of the reverse engineering process that moves from the point cloud acquisition to the virtual model reconstruction. This process is characterized by many possible settings and choices which are sometimes difficult to define and may sometimes be the cause of significant movements of the captured sample regions from the real surface. The efficiency of the entire reverse engineering cycle strongly depends on the initial point cloud characteristics, and in particular on the number of points and on their placement in the Cartesian space. For this reason, it is necessary to provide a point data set, that is a "selective sample", strictly correlated with the original scanned surface and accurately representing its morphological characteristics. In order to achieve this selective sampling solution, it is important to remember that many 3D Scanners usually acquire the object surface by using a constant grid, whose dimensions depend on the particular technology (contact, non-contact) employed [1]. Working with a wide number of possible surface morphologies, the use of the constant grid tends to cause two different scenarios: the creation of too scattered point clouds which are not suitable for working on complex zones, while scanning planes, cylinders or cone-like areas with high resolutions performances would be redundant. Considering that the common assumption "the database quality improving goes always together with the sampled point density" is not true, a sample crowded with too many points and obtained from a relatively simple surface means wider uncertainty propagation, due to the measuring tool. It is then necessary to introduce a new sentence saying that "the database quality improving is directly proportional to the propriety of the points of the cloud". Hence, considering that the acquired point density depends on the scanning resolution, whose value is locally chosen based on the surface morphological complexity, the selective sampling approach can be obtained by using an "expert" operator to locally establish which pitch is to be employed. However, in this case, the whole process would be expected to be extremely time-consuming because of possible iterations, and the final result would probably be significantly subjective.

On the other hand, the whole process can be automated by employing a morphological descriptor parameter, that can be associated with the optimal points density (or scanning pitch).

At present, the selection of the most appropriate morphological descriptor is a complex activity because different possible solutions have been provided by the technical literature. Starting from the approach that aggregates the point clouds in cluster [2] and evaluates as a morphological parameter the normal vector of its representative, it is possible to move to a new different methodology which again works with the normal vector but which evaluates it based on the local Voronoi neighbourhoods [3]. As far as the Gaussian Curvature is concerned, this parameter can be obtained by working on a point cloud and dividing it into several elementary regions characterised by a central node: the Gaussian curvature is then represented by the angular excess of the triangles converging in the central node [4]. Working with the tensor, one solution is the evaluation of this morphological parameter by using the directional curvatures and the normal vectors [5] while another makes use of the principal curvatures employing a region growing approach.

All of these methods show different strengths and weaknesses in relation to the specific geometry and application involved in. Hence, for a new user who needs to understand which approach is the one to employ, it is not always easy to understand which direction to take. Unfortunately, most of existing studies focus only on one parameter, and evaluate different operative strategies instead of giving any comparison with the other possible morphological descriptors. Moreover, a large part of the technical literature only deals with Gaussian Curvature [6].

In view of the above discussion, the present work proposes a structured comparison of the available morphological parameters, analysing different operative extraction methodologies, in order to design some preliminary point cloud management guidelines.

2.0 Morphological descriptor selection: The evaluation Method

In order to support the selection of the best morphological parameter in accordance with the specific acquisition scenario, it is necessary to define some variables able to describe in a consistent way the scenario itself.

2.1 The evaluation method: Variables

Geometrical variables and metrological performances have been analysed and evaluated by working with a survey implemented on a sample of reverse engineering users and employing a compatibility diagram approach [7]. Looking at the results of the study, three variables have been identified as key factors for the reverse engineering users for describing in a consistent way the possible working scenarios. While the first two variables depend on the object geometry, the third one is mainly correlated with the 3D scanner device. Focusing the attention on geometry, the two main variables are:

- Shape change amount
- Sharp edge number

On the other hand, as far as the parameter correlated with the 3D scanner is concerned, it is possible to synthesize the device performances by using the:

- Point cloud density

According to the value that these three variables may have, it is possible to define different morphological scenarios; each of them could be ideal or inadequate for the use of a morphological parameter and of a specific operative approach for its extraction.

In order to support this selection, before starting, it is necessary to make some considerations. First of all, considering the different dimensions of the acquirable object, it is necessary to define which is the dimension of the area over which the morphological analysis will be developed (morphological detail). This step is fundamental because morphological features have different importance depending on the extension of the object itself. The same feature can be significant over an object covering an area of 1 x 1 mm, and negligible over an object covering an area of 1000 x 1000 mm. For this reason, the value of a morphological detail cannot be absolute and universal, but only relative and, definable as 10% of the entire object area. (Fig.1).

Moreover, considering that the cited variables are described as an amount, it is necessary to define their scale. From the user point of view, the scale of all these variables can be considered as binary one, because the most frequent scenarios are characterised by: *many or few sharp edges* and *many or few shape changes*.

From this point of view, it is necessary to split the variables scales into two intervals by using a threshold. Its value can be defined as the percentage of the morphological detail areas composing the object surface characterised by shape evidences. If this value is bigger than 50%, the variable describes a scenario with significant morphological features (high complex geometry). On the contrary, if the percentage is equal or lower than 50%, the scenario will be characterized by a quite smooth shape.

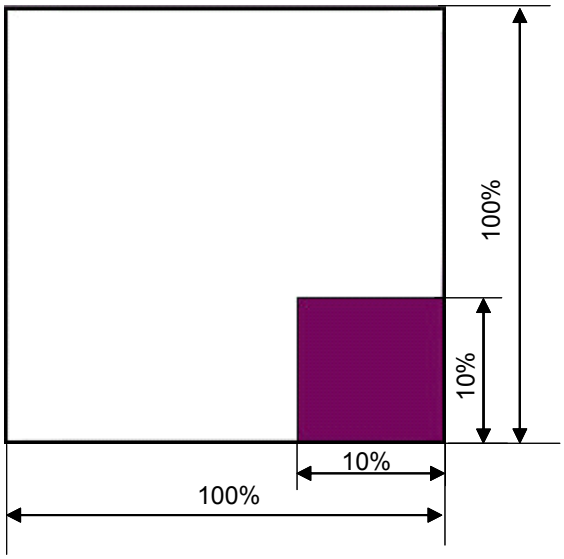

Figure 1: Point cloud elementary region

Starting from this hypothesis, it is possible to formalise the different variables necessary to synthesize the different possible working scenarios.

2.1.1 Shape change Amount

Starting from the previous hypothesis at this stage it is possible to rationally formalise the meaning of "surface with many (few) shape changes". In fact, it will mean a surface where it is possible to find at least (at most) 51% (50%) of the morphological detail squares, with at least a shape change inside. This is important for objectively codifying what an expert eye could subjectively detect as a shape change and in general as a complex (smooth) surface.

The amount of shape changes in an object geometry is identified with the help of the second derivative. The second derivative of a function gives information on the concavity of a curve. A curve variation always corresponds to a change of concavity.

First of all, the first derivative is analysed in order to study the function trend and to establish the existence of any stationary point. In order to obtain a higher precision in the function study, the second derivative analysis is also carried out assessing the presence of inflection points (points where the second derivative is equal to 0) and localising the convexity intervals.

If $f''(x) > 0$, then *f* is convex in *x*, if $f''(x) < 0$, then *f* is concave in *x*, if $f''(x) = 0$, then *x* is a point of inflection. The inflection points correspond to a change in the curve curvature.

2.1.2 Sharp edge number

It is also possible to formalise the meaning of "surface with many (few) sharp edges". Similarly to previous variable (Shape change amount) the threshold is located over the 50%. It in fact will mean a surface where it is possible to find at least (at most) the 51% (50%) of the morphological detail squares, with at least a sharp edge inside.

From a mathematical point of view, it is possible to say that a point $A = (x_0, y_0)$ of a *C* curve parameterised by the continuous function $y = f(x)$ is a cusp (or that the function *f* has a cusp at x_0) if *f* is derivable in a deleted neighbourhood and at this point, we have $\lim_{x \to x_0^-} f'(x) \neq \lim_{x \to x_0^+} f'(x)$.

Geometrically speaking, this means that at this point there are two different tangent lines, a right one and a left one.

Considering the surfaces, it is not possible to consider just one tangent because the study must be done in three dimensions. The partial derivative [8] is a first generalization of the concept of a derivative of real functions of several variables. If for real functions the derivative is the slope of the graph of a function (a

curve contained in the plan), the partial derivative at a point in relation to (for example) the first variable of a function of *x* and *y,* is the slope of the curve obtained by intersecting the graph of *f* (an area contained in the space R^3) with a plane passing through the point and parallel to the plane *y = 0*. The directional derivative [8] is a tool that generalizes the concept of partial derivative; it no longer occurs only along directions parallel to the Cartesian axis, but in any direction determined by a vector. Let $f : \Omega \to R$ (with $\Omega \subseteq R^2$ open set) be and a point $(x_0, y_0) \in \Omega$; take a unit vector $\bar{v} = (v_1, v_2)$. Then the direction derivative with respect to unit vector v of f in (x_0, y_0) is $D_v f(x_0, y_0) = \lim_{t \to 0} \frac{f(x_0 + tv_1, y_0 + tv_2) - f(x_0, y_0)}{t}$, if this limit exists finite[8].

2.1.3 Point cloud density

As far as the point cloud density is concerned, it is not necessary to talk about the threshold discussed before (50%), because of the structured grid employed (uniform point cloud). As a consequence, talking about "very crowded (sparse) point cloud", means that when working with two points P_1 and P_2 their distance is less (bigger or equal) than 10% of the length of side of the whole object area : $d(P_1,P_2)<10\%$ ($d(P_1,P_2)>= 10\%$).

2.2 The evaluation method: Euclidean Space Scenarios Formalisation

Starting from the considerations we made before, each variable could then be described on a binary scale. When working with an Euclidean space, each of them could be graphically represented by employing a three axis framework (Fig. 2). Its origin describes a scenario where the point cloud has been obtained through the acquisition of an object characterised by few shape changes, few sharp edges and low density.

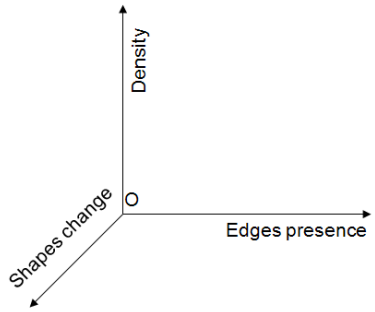

Figure 2: Euclidean framework variables layout

The three variables belong to the interval $[0,1]$ and, for handiness, they will be indicated as:

- $x =$ sharp edge,
- $y =$ density,
- $z =$ shape change.

and so $x, y, z \in [0,1]$.

These variables have been located on three orthogonal axes and could be combined each others independently. Considering that every variable moves on a binary scale, every domain shall be divided into two intervals [0,1/2] and [1/2,1] (Tab.1) (Fig.3).

Intervals / Variables	$\left[0, \frac{1}{2}\right]$	$\left[\frac{1}{2}, 1\right]$
x	**few sharp edges**	**many sharp edges**
y	**sparse point cloud**	**crowded point cloud**
z	**few shape change**	**many shape change**

Table 1: Framework variables intervals

Each combination will synthesize a possible scenario (for greater convenience, “scenario” will also be called case and combination in the next lines), where an optimal morphological parameter could be identified. In the Euclidean space the possible combinations will be located in a specific place inside a cube. The entire scenarios set is represented by a cube or side dimension 1, called “decisional cube”. On the Euclidean space each of these combinations is represented by a cube of side length ½ and which is located inside of the decisional cube.

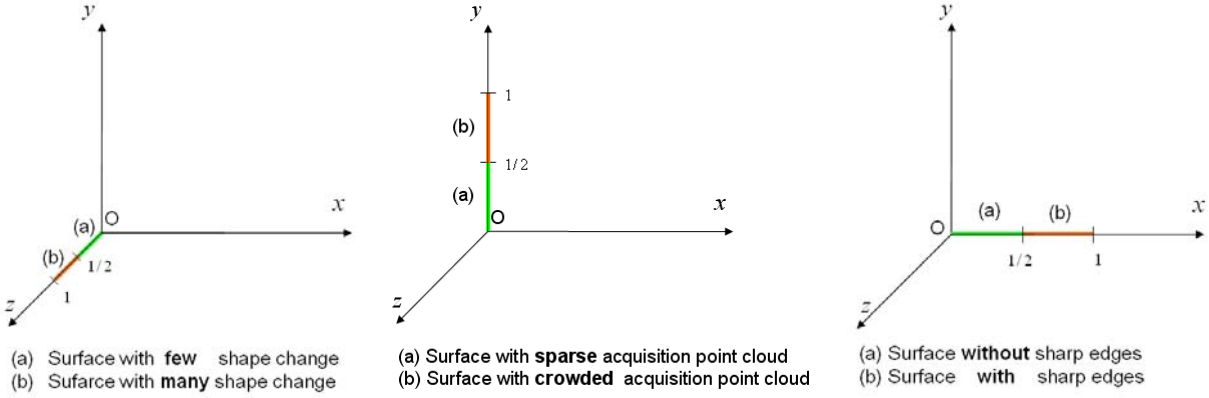

Figure 3: Framework variables intervals

In order to provide a reliable analysis about the best morphological parameter, all the possible variables values have been combined to analyse as many scenarios as possible (Tab.2).

Cases	Few shape change	Many shape change	No sharp edges	With sharp edges	Spare	Crowed	
Case 1	X		X		X		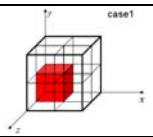
Case 2	X			X	X		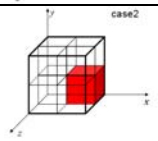
Case 3	X		X			X	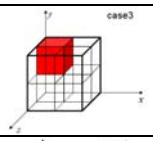
Case 4	X			X		X	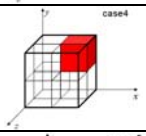
Case 5		X	X		X		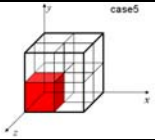
Case 6		X		X	X		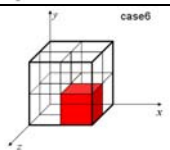
Case 7		X	X			X	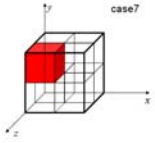

Case 8		X		X		X	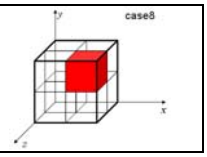

Table 2: Euclidean space scenarios representations

3.0 Morphological descriptor selection: operative extraction methodologies

Once defined the starting hypothesis and defined the comparison methodology, and before starting the structured comparison of the available morphological parameters, the key points of the morphological parameters extraction methodologies have been analysed by underlining strengths and weaknesses with respect to the possible scenarios cited before.

3.1 Morphological descriptor: Normal

The normal vector, often just called the "normal," to a surface is a vector perpendicular to it. Often the normal unit vector is preferred, sometimes known as the "unit normal". When normals are considered on closed surfaces, the inward-pointing normal (pointing towards the interior of the surface) and outward-pointing normal are usually different. An Euclidean vector at a point of a surface is normal to the surface if it is orthogonal to the tangent plane and, consequently, to every tangent vector to the surface at the point.

3.1.1 Normal: Local Voronoi Neighbourhood (Method 1)

The procedure that involves the evaluation of the normal vector usually includes the following three fundamental steps:

1. Neighbouring points identification where applying the normal vector estimation
2. Normal vector evaluation based on local neighbouring points
3. Defining the input/output direction for the normal vector

Following this method [3], it is possible to identify the local Voronoi mesh neighbourhoods of a specific point starting from the global Voronoi neighbours. At the beginning, the Voronoi diagram is created by employing the quickhull [9] algorithm, which stands out for its simplicity and its computational efficiency. After that, the Voronoi mesh neighbours have been made starting from the local triangular mesh growing algorithm as the ball-pivoting approach [3]. Once the neighbouring points have been identified, it is possible to evaluate the normal vector. This evaluation is based on the quadratic curve fitting and allows users to find the normal vector of the point P_0 starting from its K local Voronoi mesh neighbours. The key points of this procedure can be summarised through the following lines (Fig.4):

- Identifying the correspondent P_j points over the local Voronoi mesh with the biggest angle in P_0
- Fitting a quadratic curve $P(u)$ through P_i,P_0 and P_j [2]
- Extracting the directional tangent vector from the fitted quadratic curve
- Evaluating the normal vector **n** in the P_0 point [2]:
  - The s^2 variance of the **n** and K directional tangent vector dot product is evaluated.
  - Employing a manipulation method [9] it is possible to obtain a 3x3 matrix where the column vectors are eigenvectors with $\lambda_1, \lambda_2, \lambda_3$ as eigenvalues. The eigenvector correspondent to the minimal eigenvalue is the normal vector that minimizes the variance.

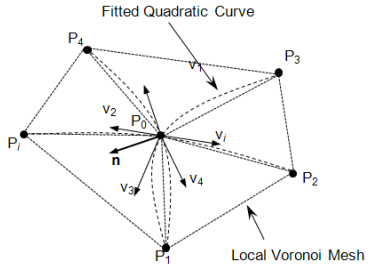

Figure 4: Normal vector **n** at P_0

The method for evaluating the normal vector **n** at P_0 is graphically shown in figure 4.

During the following steps, the normal vectors of both internal and external directions are defined in order to obtain a consistent global orientation for the normal vectors in the sampled points. For this purpose the local mesh is employed for identifying the two poles of the Voronoi cells (Tab.3) (Fig.5).

Strengths	**Weaknesses**
This approach is accurate and consistent; in fact, while increasing the sample dimension, its probability distribution converges on the estimated parameter. The normal vector evaluation method features a wide number of geometric analysis algorithms for point cloud. Moreover, the Voronoi diagram is indipendent from point cloud density and, more important, the Voronoi neibouring points form a set that reliably represents local surface geometry. The Delaunay triangular mesh is a global structure that allows users to identify the shape minimum volume 3D representation in any case. This feature allows a better shape approximation proportional to the point cloud density. Generally speaking, experimental results coming from the technical literature describe this method as robust and able to evaluate the normal vector with consistency.	The normal vector is a local geometric property. As a consequence of this, it is necessary to make a careful evaluation of the neighbouring points. In fact, by introducing too many points the local characteristic of the estimated normal vector could degrade, adding misleading information into the point cloud. However, if the point cloud is too scattered the choice of the optimal neighbouring point is strongly limited, because it is not able to provide a consistent representation of the surface geometry.

Table 3: Local Voronoi neighbourhood method strengths and weaknesses

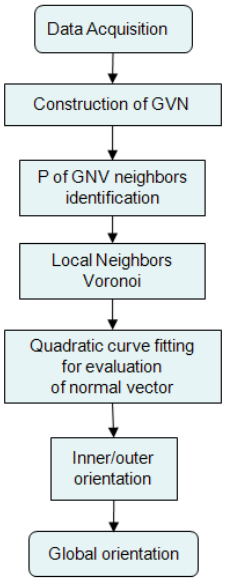

Figure 5: Local Voronoi neighbourhood flowchart

3.1.2 Normal: global clustering approach (Method 2)

This method starts from a dense point cloud formed by M points belonging to a continuous surface S. The goal of this methodology is to find a subset $P_N \subset P$ with a specified number of points $N < M$ which minimizes the geometric deviation between the surfaces represented from P_N and P [2].

This approach is divided into three fundamental steps: the objective function definition, the objective function evaluation and the objective function minimization. The definition is based on clustering and point-

to-surface distance approximation concepts. N points belonging to P are considered and named $\bar{r}_i$. They are defined as representatives. The set of $\bar{r}_i$ is P_N (Fig.6).

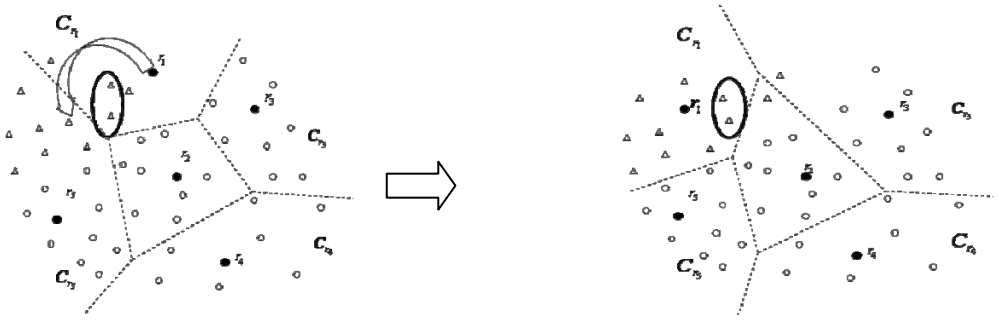

Fig. 6 Configuration change: representative $\mathbf{r}_1$ replaced by $\mathbf{r'}_1$

After that, a cluster is created with a representative $\bar{r}_i$, belonging to P_N, and every point $\bar{p} \in P / P_N$, so that the distance between $\bar{p}$ and $\bar{r}_i$ is minimum.

An objective function is defined and used to evaluate an optimal configuration for P_N, but it is not sufficient to obtain a continuous surface representation starting from the point cloud. The geometric shape of the surface S_N, represented by a simplified data set P_N, is approximated by the normal vector, which is evaluated for each point belonging to P_N. The normal vector $\bar{n}_{\bar{r}_i}$ in $\bar{r}_i \in P_N$ is evaluated by using the $\bar{r}_i$ neighbouring points in P_N [3].

Another problem that occurs frequently is that, when the P_N configuration changes (Fig.6), the cluster representation and the correspondent normal vector also change. In this approach, these changes are controlled in a predictable way and they can therefore modify the objective function. The objective function minimization process consists of two correlated steps in which the layout cluster is improved and hence the representatives choice is refined (Tab.4)(Fig.6).

Strengths	**Weaknesses**
In this approach the geometric deviation accuracy is made in a cluster-by-cluster way. Few clusters at each iteration are taken into consideration and the evaluation can be carried out in a rigorous way. It is possible to obtain a data series by varying the point number in P_N. This extracted data set will represent the input data's original geometry at different detail levels. However, the estimate requires much fewer neighbouring points (minimum three) compared to the quadratic surface fitting method that requires at least nine neighbouring points. Since the Voronoi diagram of P_N usually supplies at least three neighbouring points for every representative $\bar{r}_i \in P_N$, this method can profit from the 3D Voronoi diagram structure, which well constructed for the desired neighbouring points' choice.	The whole method is based on the assumption of a dense point cloud. It is better not to take a very small *N*, because the object function's stability is based on the point-to-surface distance approximation which, in such a case, might not be efficient enough. The problem of the relationship between point density and the approximation resulting error remains.

Table 4: Global clustering approach method strengths and weaknesses

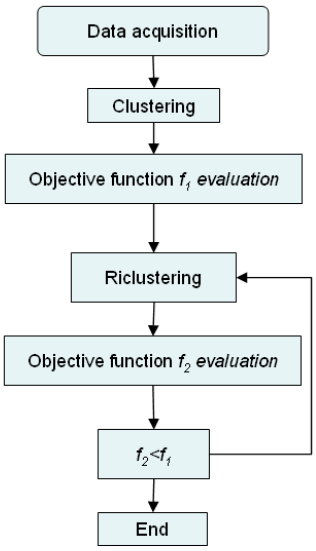

Figure 7: Global clustering approach neighbourhood flowchart

3.2 Morphological descriptor: Gaussian Curvature

When working with a generic geometry it is possible to evaluate its morphological complexity by employing two perpendicular planes cutting the surface in one point p_0. Looking at these planes, it is possible to work on two curves to analyse their geometrical behaviour. This operation provides the principal curvatures k_1 and k_2 of the two curves and on the same point. The product of these values provides the Gaussian Curvature morphological descriptor.

3.2.1 Gaussian Curvature: percentiles (Method 3)

In the methodology [10], there is a process used for parametric surfaces and another similar one for discrete surfaces. When dealing with point clouds, it is necessary to use the discrete one and therefore to work on a triangular mesh M composed by a vertex set $V=\{v_i\} \subset \mathbf{R}^3$, a edges set $E=\{e_j=v_{j1}v_{j2}\}$ which connect the vertexes and a triangles set $T=\{t_k=\Delta v_{k1}v_{k2}v_{k3}\}$. The incident angles in v_i are defined as $\{\alpha^i_1, \alpha^i_2, \ldots, \alpha^i_{di}\}$ where d_i is the vertex degree v_i (Fig.8).

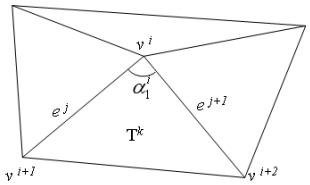

Figure 8 : Vertex and related variables

As a consequence of this, the Gaussian curvature K^T [10], used in the differentiable surfaces, can be approximated in the discrete ones as the sum of the K_i^T in each vertex in a specific region. Hence, in a specific vertex v_i the curvature integral can be approximated from [12,4]: $K_i^T = \int_S^{Kds} \approx 2\pi - \sum_{j=1}^{j=d_i} \alpha^i_j$.

Considering that for discrete surfaces the Gaussian curvature K_i^T is only an approximated value, the presence of noise during the data acquisition process and of geometric and topologic features embedded in the mesh can lead up to misleading information.

The cover surface boundary [10] and the associated topological features often result in edges not shared with the other two triangles (Fig.9).

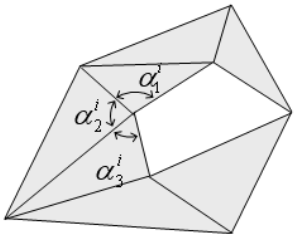

Figure 9 : Degenerate vertex due to a specific feature (hole)

In this case, the smooth surfaces curvature is not well defined. For the vertices in this case, the K_i^T values, computed by the integral, are directly linked to the boundary curve's curvature instead than only to the surface curvature. These vertices, whose computed K_i^T value cannot represent the surface shape, are defined as degenerate vertices. In fact, once defined the threshold value, $K_e = 2\pi/3$, if the vertices satisfy $K_i^T < K_e$ they are erased.

On the basis of the computed values, a 2D spherical map is designed. With K_i^T it is possible to evaluate the curvature associated with (x_i, y_i) and with r_i and the distance from the center. The vertices are then grouped together on the basis of the percentile and divided into n concentric regions. For each region *j*, the integral of the Gaussian curvature K_j^T is calculated as the summation of all the K_i^T, namely $K_j^T = \sum_{i \in I_j} K_i^T$. For each input it is possible to obtain a vector **K=**[$K_1^T, K_2^T, .., K_n^T$] that represents the curvature integral of every concentric region.

The similar meshes are then compared by means of some correlation coefficients. The values of these coefficients will correspond to a high or low similarity level (Tab.5)(Fig.10).

Strengths	**Weaknesses**
One of the main advantages provided by the method is the efficient computational behaviour. Because of the use of a two meshes comparison, when analysing the different morphological behaviour of the two geometries, the calculation of the curvature integral is reduced to the comparison of the **K** values in pair; from a computational point of view, this process is equivalent to comparing two vectors. This methodology includes both continuous and discrete models approaches.	The proposed methodology is suggested for freeform surfaces. In fact, it is not applicable to the study of prismatic geometries or complicated topologies with flat geometries because there are many degenerate vertices. When working with discrete surfaces, the Gaussian curvature value provided is just an approximation which highly depends on the mesh quality. In fact, big mesh size and layout variations could lead to incorrect conclusions. According to this methodology, another limitation in the use of this parameter is the density of the point cloud. The approximation of the Gaussian curvature integral through the formula mentioned above, leads to satisfying results if the sample is sufficiently large.

Table 5: Percentiles method strengths and weaknesses

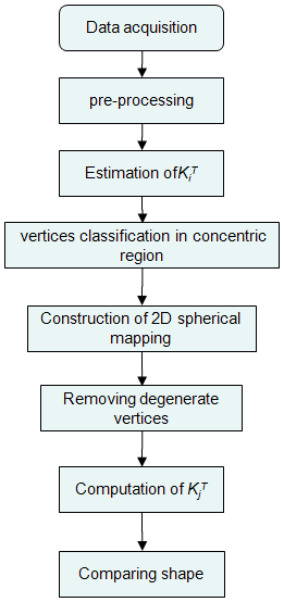

Figure 10: Percentiles method flowchart

3.2.2 Gaussian Curvature: angle deficit in spherical image (Method 4)

The curvature of a surface can be approximated with another method that has been developed starting from the Rodriguez Theorem [13]. The surface is approximated by a polyhedron with triangular faces whose vertices are the points of the surface. For example, point 0 is surrounded by the triangular faces P_iOP_{i+1} (Fig.11). The spherical image of the polyhedron is a set of points of the unit sphere (the head of the unit vectors parallel to $n_{i,i+1}$). These points are linked by arches and a spherical polygon is created on the unit sphere.

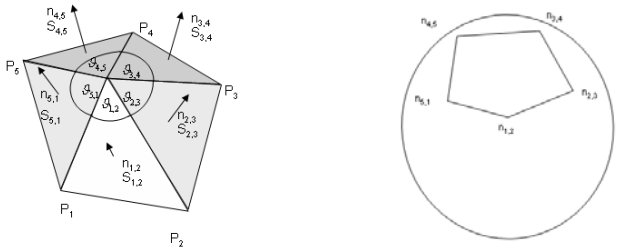

Figure 11: Angle deficit method

The area of the spherical polygon is the angle deficit of the polyhedron [11], $2\pi - \sum \vartheta_{i,i+1}$. The area of each triangular face of the polyhedron can be subdivided into three equal parts, one for each vertex, so that the area relative to point ***O*** on the polyhedron is $\frac{1}{3}\sum S_{i.i+1}$. This value is considered as an approximation of the area of the curve on the surface around ***O,*** although the curve has not been specified. Hence an approximation of the curve in ***O*** is

$$K = \frac{2\pi - \sum \vartheta_{i,i+1}}{\frac{1}{3}\sum S_{i,i+1}}.$$

This formula for calculating ***K*** is for example used by [6,14,15,11] (Tab.6)(Fig.12).

Strengths	**Weaknesses**
In order to obtain the best curvature approximation with this method, it is necessary to have a very high point cloud density sample. Furthermore, from	The curvature approximation with the angle deficit method has proved to be not too accurate at times. For uniform and not uniform data, the angle deficit

a computational point of view , this methodology is highly indicated for free-form surfaces.	method is able to approximate the curvature with precision O(1). It has been shown that for high point cloud sample density other known methods lead to a higher approximation error, because the method is independent by the points distance.

Table 6: Angle deficit method strengths and weaknesses

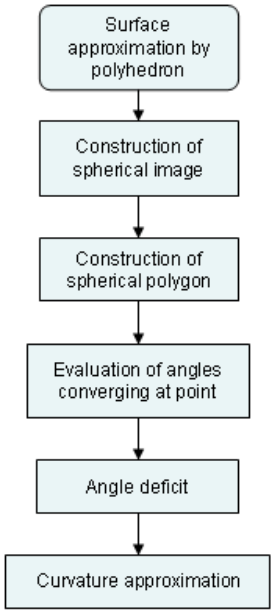

Figure 12: Angle deficit method flowchart

3.2.3 Gaussian Curvature: quadratic surface fitting (Method 5)

This method provides a curvature approximation starting from a quadratic interpolation surface. The normal and the curvature of a quadratic surface can, in fact, approximate the normal and the curvature of a surface.

A quadratic surface that passes through the origin is given by

$$z=A_{10}\,x+A_{01}\,y+\frac{A_{20}}{2}\,x^2+A_{11}\,xy+\frac{A_{02}}{2}\,y^2\ . \qquad (1)$$

It is required to pass through other five points as well. Considering the points (X_i,Y_i,Z_i), $i=1,\ldots,5$ it is possible to express this condition through the following system:

$$\begin{pmatrix} X_1 & Y_1 & \frac{X_1^2}{2} & X_1Y_1 & \frac{Y_1^2}{2} \\ \cdots & \cdots & \cdots & \cdots & \cdots \\ X_5 & Y_5 & \frac{X_5^2}{2} & X_5Y_5 & \frac{Y_5^2}{2} \end{pmatrix} \begin{pmatrix} A_{10} \\ A_{01} \\ A_{20} \\ A_{11} \\ A_{02} \end{pmatrix} = \begin{pmatrix} Z_1 \\ Z_2 \\ Z_3 \\ Z_4 \\ Z_5 \end{pmatrix} \qquad (2)$$

If system (2) has a unique solution, it is possible to find the curvature through this method. The curvature of the quadratic equation (1) will be given by:

$$K=\frac{A_{20}A_{02}-A_{11}^2}{L^2}\text{, where } L=A_{10}^2+A_{01}^2+1\,.$$

The form of the quadratic formula can be extended including the terms in x^2y, xy^2 and x^2y^2 [4]. In this case eight points will be necessary and a system of 8x8 linear equations will be the result (Tab.7)(Fig.13).

Strengths	**Weaknesses**
This method works for both uniform and not uniform data giving an approximation O(h) of the curvature. This means that the method has a linear dependence on the point distance inside of the point clouds. Besides, experimental results coming from the technical literature show that the distance between points, and also the density of the point cloud, do not excessively affect the surface approximation. Whenever the surface can be classified as a free-form surface, the approximation provided by this method supplies very good results thanks to the absence of significant irregularities.	Working with a fitting quadratic equation (1), the method involves matrices representation (2). For this reason, if these are badly conditioned the method could provide poor accuracy results. If this method is used for not free-form surface, the process of fitting the quadratic equation could supply misleading results and, as a consequence, the curvature approximation is likely to have a level of inaccuracy proportional to the irregularities presence. In fact, the use of this methodology is not recommended when the geometry is characterised by a lot of sharp edges.

Table 7: Angle deficit method strengths and weaknesses

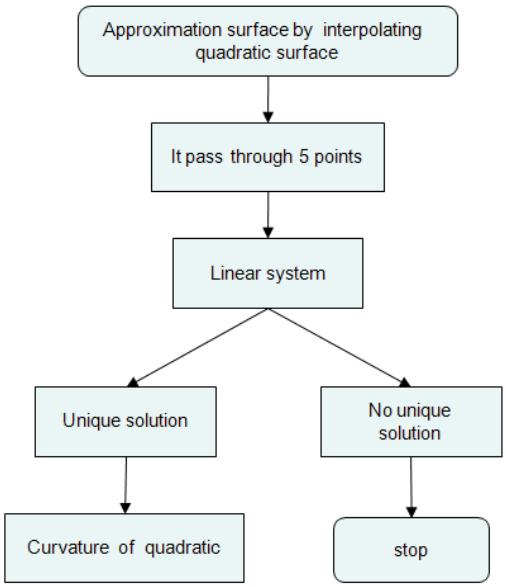

Figure 13: Angle deficit method flowchart

3.3 Morphological descriptor : curvature tensor

The curvature tensor of a surface *S* is the map $p \mapsto k_p$ that assigns to each point *p* of *S* a function measuring the directional curvature $k_p(T)$ of *S* in *p* in the direction of the unit vector *T*, tangent to *S* in *p*. The curvature tensor is representable through a 3x3 symmetrical matrix *M*. Its eigenvalues are k_1 , k_2 , 0 and the correspondent eigenvectors are **k_1, k_2,** *N*. k_1 and k_2 represent the principle curvature; **k_1 and k_2** the correspondent principle directions; and *N* the normal to the area. *M* is interpretable as the normal vector variation in small neighbourhoods. Hence, the necessary information is available for building *M* as $M=PDP^{-1}$ with

P=(k1, k2,) e D= $\begin{pmatrix} k_1 & 0 & 0 \\ 0 & k_2 & 0 \\ 0 & 0 & 0 \end{pmatrix}$.

3.3.1 Curvature tensor: based on Normal Cycle (Method 6)

This is an efficient algorithm [16] to decompose a triangulated mesh. It is based on the curvature tensor field and it consists of two complementary steps: 1) a region based segmentation, which is an improvement of what was already computed by Lavoue and others [17] and that decomposes the object into several patches with a constant curvature; 2)a boundary rectification based on curvature tensor directions, that corrects the boundaries and eliminates their artefacts or discontinuities. An original method of segmentation is presented to decompose an original 3D mesh into patches characterized by a uniform curvature and clear boundaries. The simple and efficient classification identifies any curvature transition; hence, it allows to segment the object into confining regions with constant curvature without cutting the right object in its sharp edges.

In the first step, *curvature based region segmentation*, a pre-processing step identifies sharp edges and vertices; the curvature tensor is then calculated for each vertex according to the work of Coree- Steiner et al. [18], based on the Normal Cycle. Vertices are classified into clusters, according to the principal curvature values *Kmin* and *Kmax*. With the help of a region-growing algorithm, the triangles are assembled into connected labelled regions according to the vertex clusters. Finally, a region adjacency graph (RAG) is processed and reduced in order to merge similar regions according to several criteria (curvature similarity, size and common perimeter).

During the second step, *boundary rectification*, boundary edges are extracted from the previous region segmentation step. Then, for each of them, a boundary score is calculated which notifies a degree of correctness. According to this score, estimated correct boundary edges are marked and used in a contour tracking algorithm to complete the final boundaries of the object (Tab.8)(Fig.14)

Strengths	**Weaknesses**
The procedure used to estimate the tensor provides satisfactory results even for not well tasselled objects. It is independent from acquired point cloud density and offers the possibility to filter noised objects. The fact of working with the orientation of the curvature tensor allows to eliminate "artefacts". The density of the cloud does not influence the algorithm efficiency because, in the presence of a too crowded point cloud, the method itself carries out a selection of the optimal neighbouring points, excluding those that are considered superfluous for the surface segmentation. If the cloud is sparse, the problem is solved through the region growing process.	This methodology involves a significant computational cost due to its several passages, but it does not provide significant weaknesses. The presence of many steps could cause loss of information or error dispersion and for this reason, when working with free-from surfaces, there are other more efficient solutions.

Table 8: Tensor method strengths and weaknesses

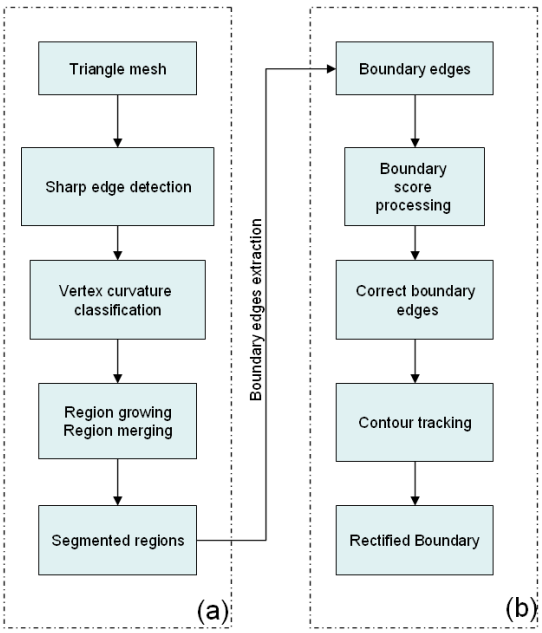

Figure 14: Normal cycle method flowchart .
(a) constant curvature region segmentation, (b) Boundary rectification

3.3.2 Curvature tensor: approximation matrix for tensor evaluation (Method 7)

To analyse the curvature tensor, the matrix M_p is defined with an integral. This matrix has the same eigenvectors as K_p [5], and its eigenvalues are connected to a few linear homogeneous transformations. The computation of the curvatures and of the principle directions of S in p derives from the diagonalization of the matrix M_p, which can be obtained in closed form. A scheme of finite differences is then used to approximate the directional curvatures [5]. If q is another point belonging to the surface S, close to p, and *t* is the normalized projection on the tangent plane $\langle N \rangle^T$ of the vector $q-p$, the directional curvature can be approximated as follows $k_p(T) \approx \frac{2N^t(q-p)}{\|q-p\|^2}$ (3).

In this method a polyhedron is considered as an approximation of the unknown surface. Only triangulated areas are considered, both closed and limited, but supposedly orientated and consistent [20].

The first goal is to evaluate the normal vectors. As explained in [19], the faces of the surface are planar, every face f_k has a normal unit vector N_{f_k}. The normal in the vertex v_i is defined as the normalized weighted sum of the normals incident into the faces, with a weight proportional to the surface face areas [19]. The second aim is to calculate the matrix M_{v_i}, approximating it with a summation of weighed sums on the neighborhoods of V_i : $\widetilde{M}_{v_i} = \sum_{v_j \in V^i} w_{ij} k_{ij} T_{ij} T_{ij}^t$.

For each neighbouring point v_j of v_i, it is possible to define T_{ij} as the normalized projection of the vector $v_j - v_i$ on the tangent plane $\langle N_{v_i} \rangle^{\perp}$ [19]. It is now possible to approximate the directional curvature $k_{v_i}(T_{ij})$ using the formula of the equation (3).

The weights are chosen proportionally to the sum of the areas of all the rectangles of the surface that are incident both in the vertex v_j and in the vertex v_i. Therefore $\sum_{v_j \in V_i} w_{ij} = 1$.

The normal vector N_{v_i} is an eigenvector of the matrix $\widetilde{M}_{v_i}$ associated to the eigenvalue 0. The principal curvatures are directly obtained from the two correspondent eigenvalues of $\widetilde{M}_{v_i}$, by using the appropriate formula [4].

To compute the two remaining eigenvectors and eigenvalues it's necessary to restrict the matrix $\widetilde{M}_{v_i}$ to the tangent plane $\langle N_{v_i} \rangle^{\perp}$ using Householder transformation [20]; after that, the resulting 2x2 matrix must be diagonalized in closed form with a Givens rotation [20]. In this way, the computed principal directions have to be orthogonal to the normal vector N_{v_i}, even if one of the values of $\widetilde{M}_{v_i}$ is zero, or close to zero.

It is possible to obtain an angle ϑ so that the vectors $T_1 = \cos(\vartheta)\widetilde{T}_1 - \sin(\vartheta)\widetilde{T}_2$ and $T_2 = \sin(\vartheta)\widetilde{T}_1 + \cos(\vartheta)\widetilde{T}_2$ are the remaining eigenvectors of $\widetilde{M}_{v_i}$, or the principal directions of the surface in v_i. The principal curvatures are obtained from the two corresponding values of $\widetilde{M}_{v_i}$, using the defined equations [19].

Finally, a pre-processing smoothing step is required for surfaces with noises, due to measuring errors or systematic problems. (Tab. 9) (Fig.15)

Strengths	**Weaknesses**
The algorithm complexity is linear, both in time and space, as a function of the number of vertices and faces of the polyhedral surface. All calculations are simple and straightforward. Expensive numerical iterative algorithms are not necessary, even for the calculation of eigenvectors and eigenvalues of the matrices involved. The experiments performed [11] show that the accuracy of this algorithm is not worse than that of other algorithms available, in some cases it is instead even better.	As any other method working with the estimation of principal directions, even this approach could provide a not reliable behaviour. In fact, if the two remaining eigenvalues of $\widetilde{M}_{v_i}$ are equal, the principal directions cannot not uniquely determined.

Table 9: Matrix tensor method strengths and weaknesses

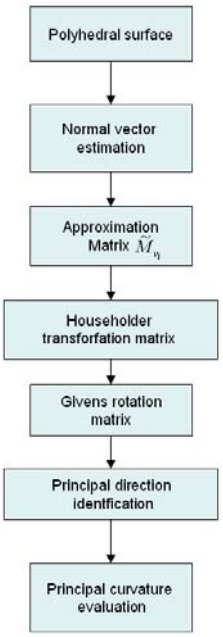

Figure 15: Matrix tensor method flowchart

4.0 The evaluation Method: Implementation

This paragraph analyses the different combinations presented above (Tab.2). In each of these cases, one or more of the methods previously described can be used. Some methods are usable in many situations, while other methodologies are not highly recommended in any of these combinations of variables. To get a more complete picture of the method applicability it is not sufficient to point out which is the best method in a given case, but rather to highlight what are the cases where a particular method cannot be used.

4.1 Implementation: Occupied positions

Different coloured little cubes have been used to highlight the cases in which a parameter can be the best morphology descriptor *(Gaussian Curvature: Yellow – Tensor: Light Blue – Normal: Violet)*(Tab.10).

CASE	SCENARIO DESCRIPTION	POSITION ON EUCLIDEAN SPACE
1	This combination simulates an ideal free-form surface. In fact it has only few shape changes and few sharp edges. Moreover, here the acquisition device has provided a quite sparse point cloud. The methods employing the Gaussian curvature are able to provide the most efficient and reliable results, because they do not require dense point cloud in order to provide good performances. Besides, a surface without sharp edges represents the ideal applicability scenario because the method is not able to manage this kind of surface features.	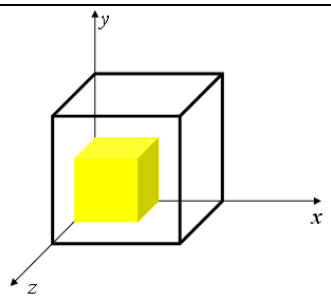
2	This scenario shows a geometry characterised by sharp edges, few shape changes and low points density. Since we are here working with geometries characterised by sharp edges, the best morphological parameter to use is the tensor. Besides, a special attention must be paid to the triangular growing method because it is able to remove reliably spikes coming from anomalous point cloud management, and to provide good performances both with few or many points and both for few or many shape changes.	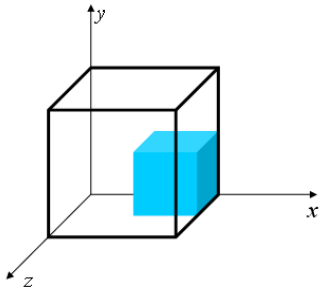
3	This scenario represents the ideal situation where there are few sharp edges, many points and few shape changes. The surface representation will be the most accurate one and for this reason all of the cited morphological descriptor are able to provide reliable information.	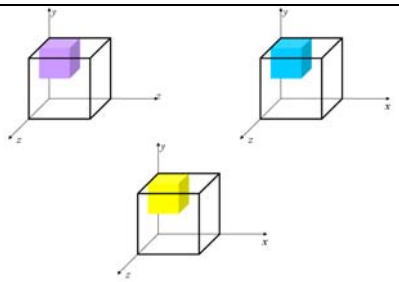
4	Here the point cloud is crowded, there are many sharp edges and few shape changes. The presence of many sharp edges imposes the use of almost all the morphological descriptors rather than the tensor. It provides the most reliable performances and it is independent by the points density and shape change amount.	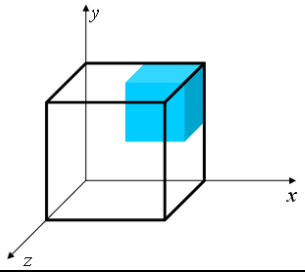

5	The presence of few sharp edges and the many shape changes suggest the use of the Gaussian curvature with specific attention to the percentiles method. This method can in fact provide the best performances when working with smooth surfaces by collecting points according to their curvature, and without limiting its applicability with respect to the shape change amount.	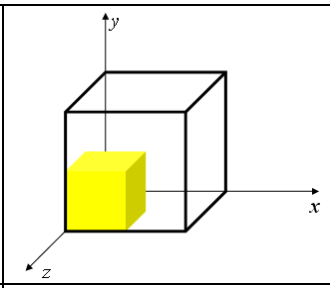
6	The presence of many sharp edges impose the use of almost all of the morphological descriptors rather than the use of just the tensor. It provides the most reliable performances and it is independent by the points density and shape change amount.	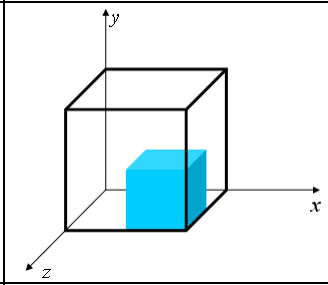
7	This case is characterized by many shape changes, crowded point cloud and few sharp edges; hence, the best solution is here provided by the use of the normal vector. In this specific scenario, and generally speaking when working with many points, the method that is able to guarantee the best performances is the cluster approach. This method is employable independently from the sharp edges amount.	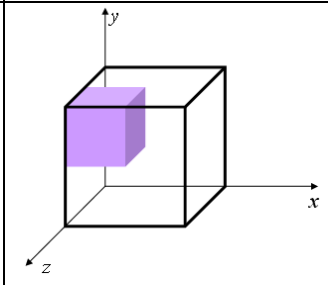
8	Here, we are dealing with a high points density, many sharp edges and many shape changes: it is therefore possible to employ the normal vector while implementing the cluster method. In this scenario this method provides optimal results.	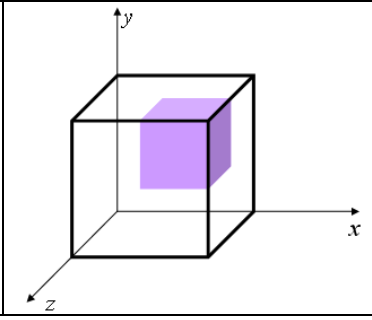

Tab.10 Euclidean space parameters positions.

4.2 Implementation: Covered areas

By locating all the cubes of the same colour in one single cube, we obtain the “decisional cube”. This cube describes all the scenarios where a single parameter can be optimal and where it doesn’t assure and optimal behaviour but it is anyway applicable because providing acceptable results. Only in case 3 (Tab.10), which can be considered as the ideal scenario, with few shape changes, not many of sharp edges and a dense point cloud, all of the already described parameters and methods can provide optimal results. For this reason, in the next lines case 3 will be considered and attention will be focused only on the other more complex cases.

4.2.1 Gaussian Curvature

The surface described in case 1 (Tab.10) is characterized by few shape changes, absence of sharp edges and a low density point cloud. In such a case the percentile method that uses the Gaussian curvature seems to be the most appropriate one. In fact, part of the methodology used in this case requires the elimination of degenerate vertices from the study, which in other words means that those vertices having a Gaussian curvature higher than a certain predetermined level must not be taken into account. Hence, a surface presenting sharp edges cannot be analysed with this type of approach, because many points would be automatically excluded from the analysis losing a significant portion of the surface geometrical behavior.

Even in case 5 (Tab.10), where the considered surface is characterized by many shape changes, absence of sharp edges and a low density cloud, it is possible to use the percentile approach (Fig16a).

By considering also the cases where the Gaussian curvature is applicable but doesn't assure the best results, it is possible to conclude that this parameters is adoptable where the geometry doesn't include sharp edges. However, there are no problems for those geometries characterised by different level of shape changes. Point density does not narrow the use of this parameter (Fig.16b).

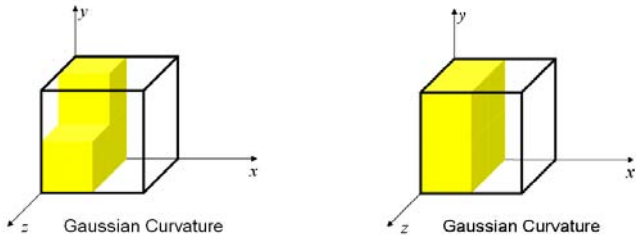

a) b)

Figure 16 : Gaussian curvature. a) optimal area, b) total area

4.2.2 Tensor Curvature

When working with sharp edges, the most suitable parameter seems to be the tensor with specific attention to the "based on normal cycle method" [16]. In fact, this method allows to segment the point cloud according to the real boundaries of the surface and then to subdivide it into several patches on the basis of the curvature. The use of this approach allows not to underestimate or neglect the presence of sharp edges leading to a not optimal final approximation of the surface. This situation occurs because when simulating the manual segmentation the method is able to handle the singularity points due to the presence of sharp edges.
In the he cases 2,4 and 6 (Tab.10) the represented geometries are characterized by many sharp edges. For this reason, in these cases the parameter that better locates the different morphological complexity areas is the tensor. Moreover the use of this parameter is indipendent by the points number in the cloud and by the presence of shape changes (Fig.17a).

From the developed analysis it appears that the tensor is a parameter that can be used in every case. It hasn't particular weaknesses or, anyhow, its use never leads to erroneous conclusions if used in the right way(Fig.17b).

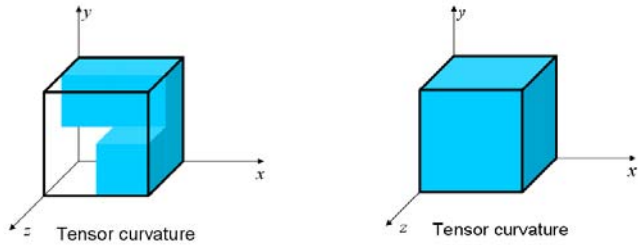

a) b)

Figure 17 : Tensor curvature: a) optimal area, b) total area

4.2.3 Normal

With high precision devices, it is possible to obtain a high density point cloud. In these cases the use of the normal provides optimal results adopting the cluster segmentation approach. This method relies on the minimization of a function dependent on a subset of points belonging to the acquired point cloud. It's necessary that the number of starting points is not too low, otherwise a subset adequate to our goal would result excessively small and there would be the risk of obtaining a non optimal result, or a result too far from reality. For this reason, it is necessary to use this approach for cases 7 and 8, characterised by the presence of a very high density point cloud. This methodology is able to well approximate significant shape changes. Furthermore, thanks to its stability, it works very well both in the presence of sharp edges and in the absence of these features (Fig.18a).

The use of the normal vector is not recommended in situations in which the point cloud acquisition instrument cannot provide a high amount of points related to the surface analyzed (low density), but does not

present any problem regarding the surface geometry. Significant or negligible shape changes and the presence or absence of sharp edges do not influence the use of this method (Fig.18b).

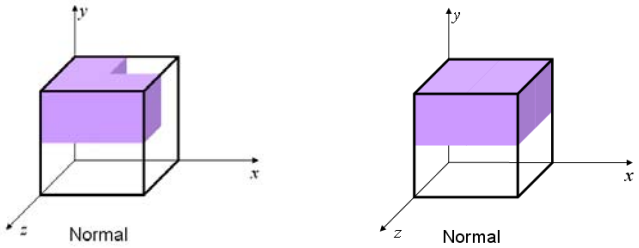

Figure 18 : Normal: a) optimal area, b) total area

4.3 Experimental validation: case studies

In order to verify the efficiency of the methodology previously introduced, four case studies have been analyzed. For each of the objects represented in Fig.20,21,22,23 the ideal geometries and their point clouds, coming from the same 3D scanner (Roland Picza)[21], have been adopted for the experimental validation.

Through the Gaussian curvature function [22] it has been possible to subdivide every surface into areas with different morphological complexities. Once obtained the original parametric surfaces, it has been possible to compute the Gaussian curvature, whose value varies according to the points *p* belonging to the surface. By analysing this function, the different morphological zones, characterising the curvature map of the selected geometries have been identified with a specific set of colours (Fig. 19).

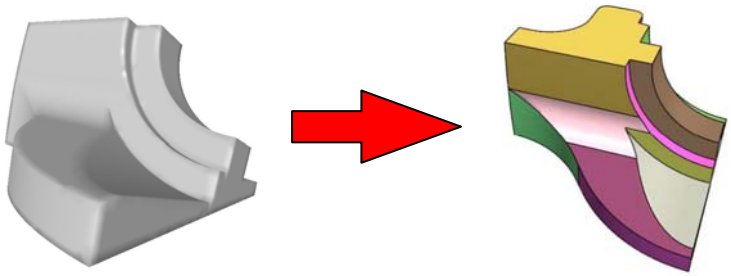

Figure 19: Fandisk and its curvature areas map

The obtained surface curvature can be classified into one of the following three groups: positive, negative or null value. Geometrically speaking, since the Gaussian curvature can also be interpreted as the product of the two principal curvatures, it depends on the maximum and minimum value of the normal curvatures. The surface zones with different Gaussian curvatures are therefore identifiable collecting those points with the same curvature in confining areas, whose borders are given by the points in which the curvature is null. In fact, since the curvature varies with continuity on the surface, when passing from negative values to positive values, bordering points, in which the curvature is null, have to exist. These are the points that define the areas to identify. A clear example of this situation is the Torus (Fig.20) in which two curvature types are identifiable: the external one with a positive value, and therefore defined as elliptical, and the internal one with a negative value, defined as hyperbolical. The points unifying these two zones are the points in which the curvature is null and are indicated in red in figure 20.

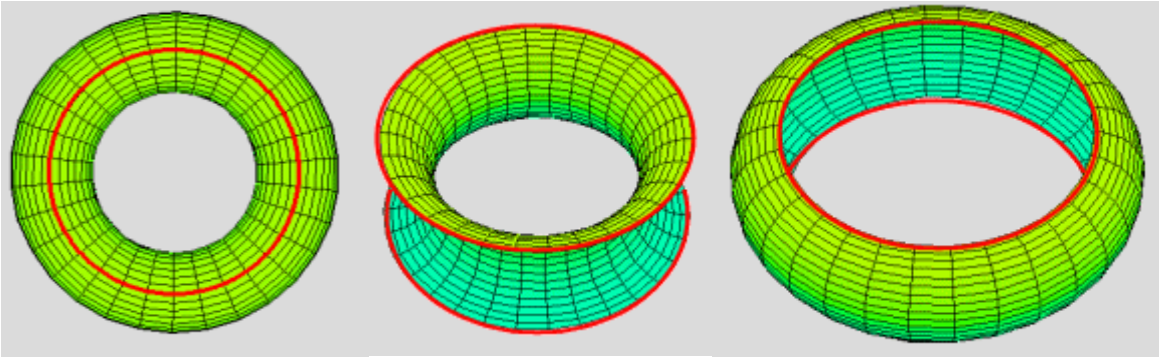

Figure 20: Torus: boundary points example

Subsequently the methodologies described in the previous sections have been applied to the point clouds obtained from the objects in figures 22,23,24,25, in order to identify, through the parameter used in each one of them, the various morphological differences inside of the surface itself. The zones with a different morphological complexity have been evidenced to distinguish them by using different colors. It is possible to see an example of this application in figure 21, where the different approaches provide a different subdivision of the surface into these zones.

Once obtained the curvature maps over the ideal parametric surfaces, these have to be compared with those coming from the available discrete methods, described in the previous paragraph , in order to identify the best matching and, as a consequence, the most efficient method for the specific point cloud and scenario (shape changes and sharp edges amount and density).

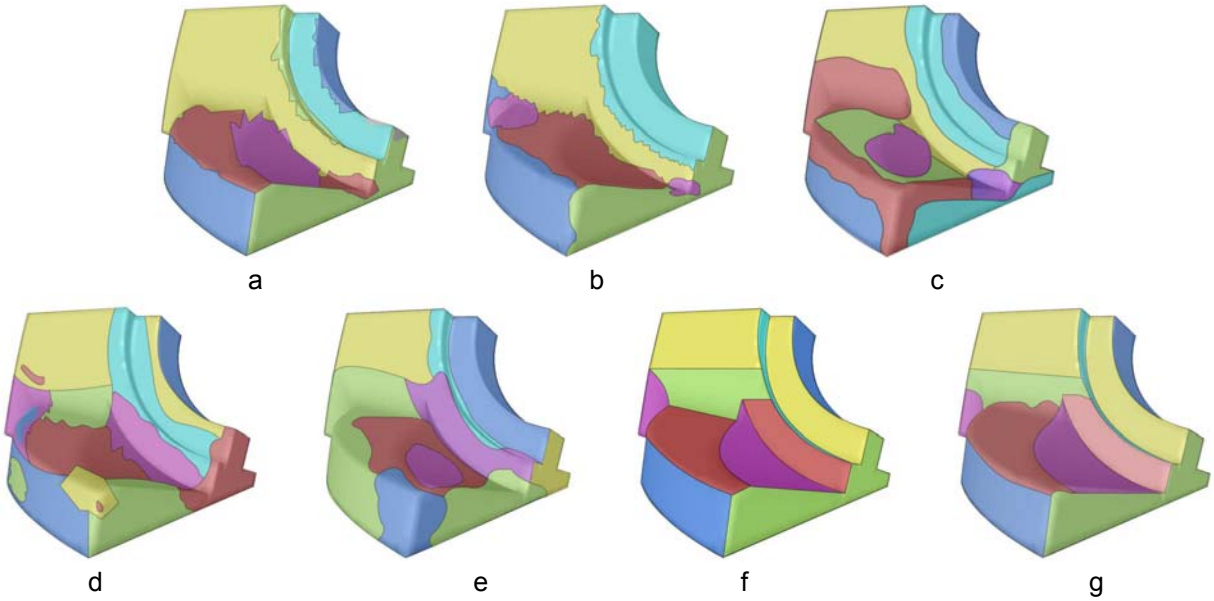

Figure 21 : Experimental results: a) method 1, b) method 2, c) method 3,
d) method 4, e) method 5, f) method 6, g) method 7

The results coming from the experimental validations have been analyzed by employing the following parameters:

- **Correspondence**: it identifies the correspondence percentage between the zones identified on the ideal geometry and those on the point clouds by the validated methods
- **Non-existent zones**: it identifies the non-existent zones parentage, anomalies coming from the use of the validated methods, differing from the Gauss map.

Sometimes the methods were able to clearly identify the areas characterized by different complexities. These zones not identifiable by the curvature function were due to an erroneous interpretation of the acquired data (Tab.11,12,13,14).

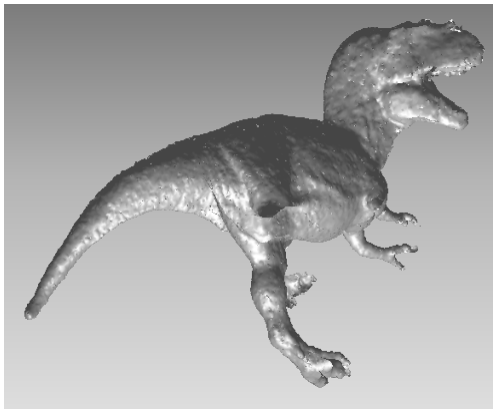

Figure 22: First benchmark

Methods	Correspondence	Non-existent zones
Method 1: Normal	95 %	-----
Method 2 : Normal	98 %	-----
Method 3 : Gaussian c.	71 %	4 %
Method 4 : Gaussian c.	65 %	7 %
Method 5 : Gaussian c.	71 %	5 %
Method 6 : Tensor c.	72 %	5 %
Method 7 : Tensor c.	68 %	7 %

Table 11: First benchmark experimental results

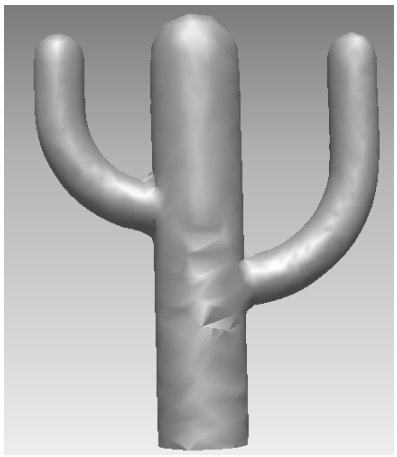

Figure 23: Second benchmark

Methods	Correspondence	Non-existent zones
Method 1: Normal	56 %	11 %
Method 2 : Normal	55 %	9 %
Method 3 : Gaussian c.	98 %	-----
Method 4 : Gaussian c.	97 %	-----
Method 5 : Gaussian c.	99 %	-----
Method 6 : Tensor c.	71 %	5 %
Method 7 : Tensor c.	79 %	4 %

Table 12: Second benchmark experimental results

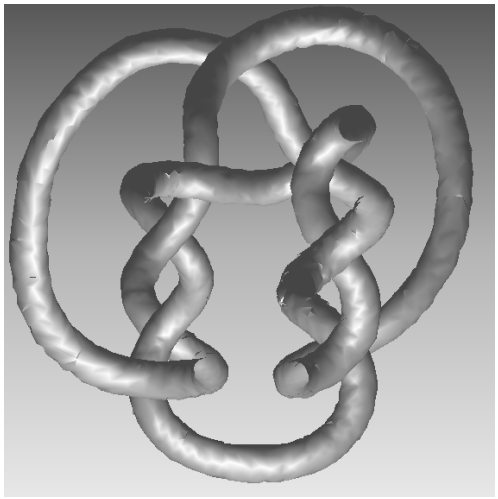

Figure 24: Third benchmark

Methods	Correspondence	Non-existent zones
Method 1: Normal	%	11 %
Method 2 : Normal	55 %	9 %
Method 3 : Gaussian c.	99 %	-----
Method 4 : Gaussian c.	97 %	-----
Method 5 : Gaussian c.	98 %	-----
Method 6 : Tensor c.	85 %	2 %
Method 7 : Tensor c.	79 %	4 %

Table 13: Third benchmark experimental results

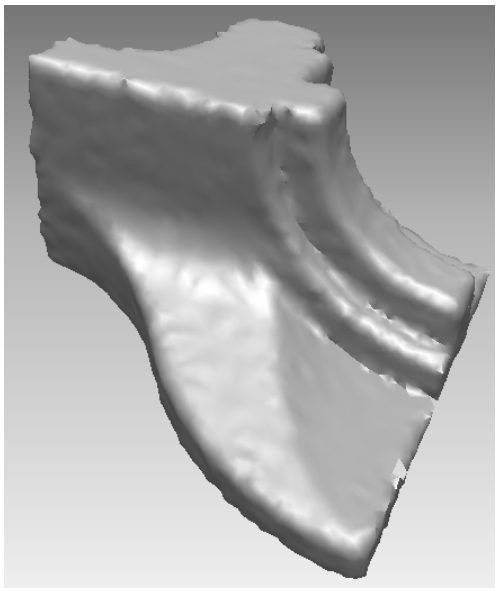

Figure 25 : Fourth benchmark

Methods	Correspondence	Non-existent zones
Method 1: Normal	64 %	5 %
Method 2 : Normal	59 %	9 %
Method 3 : Gaussian c.	71 %	40 %
Method 4 : Gaussian c.	65 %	37 %
Method 5 : Gaussian c.	71 %	35 %
Method 6 : Tensor c.	99 %	-----
Method 7 : Tensor c.	98 %	-----

Table 14: Fourth benchmark experimental results

The percentage of non existing zones does not depend on the correspondence percentage. In fact, in some scenarios, the methods employed have not been able to provide accurate borders of the areas in which the surface has been divided; however, they don't create new borders and therefore new areas. Some other times the borders can instead result being quite accurate in specific zones, but, in these cases, they also create new areas, thus increasing the percentage of non existing areas.

5.0 Conclusions

The morphological analysis of a surface cannot be carried out without subdividing the point cloud into subsets characterized by the same morphological complexity. As yet we are not able to implement this with a universal parameter and methodology; however, there are many different solutions, strongly correlated with the specific context where they can be applied. It is quite complex for new users to understand which could be the best parameter for their application.

To address this issue, we proposed and verified a series of guidelines to support the identification of the best parameter and method according to each specific application.

Firstly, a variable set, composed by acquired geometry and the acquisition device parameters, has been introduced in order to describe the possible working conditions that users could find with respect to the application they are involved in.

In the next step, all the possible working scenarios have been identified and described by combining all the identified device and geometry variables identified.

By combining the different morphological parameters *(curvature tensor, Gaussian curvature, …)* and methods (*normal cycle, percentiles, …*) with the different working scenario identified, it has then been possible to extract the strengths and weaknesses of the parameters and methods in the specific scenario.

Collecting all these data, a complete set of guidelines for supporting the selection of the best morphological parameter and method have been formalised with the support of a graphical visualisation (decisional cube).

During the process, some benchmarks have been used for validating the proposed guidelines, and for comparing the results obtained by applying the analyzed methodologies to benchmark point clouds, with the results obtained by using the corresponding ideal surfaces.

From a general point of view, it is hence possible to say that the tensor appears to be the most universal parameter, because it is able to provide acceptable results in every scenario. Nevertheless, the normal vector and the Gaussian curvature are able to provide better performances than the tensor in some applications.

6.0 Acknowledgments

The author wants to thank Miss. Pamela Moschini for the valuable suggestions and help provided during the development of this research work.

7.0 References

[1] Bidanda B, Harding K., (1991) “Reverse Engineering: an Evaluation of prospective non contact technologies and applications in manufacturing systems”, Int. J. Computer Integrated Manufacturing, Vol 30, No 10, pp.791 – 805.

[2] Hao Song, Hsi-Young Feng. A global clustering approach to point cloud simplification with a specified data reduction ratio.Comp-Aided Des; 2008; 40:281-292

[3] Daoshan Ou Yang, Hsi-Yung Feng. On normal vector estimation for point cloud data from smooth surfaces; Comput-aided Des; 2005; 37:1071-1079

[4] D.S. Meek, D.J.Walton. On surface normal and Gaussian curvature approximations given data sampled from a smooth surface. Comput-Aided Geom Des; 2000;521-543

[5] Gabriel Taubin, Estimating the tensor of a surface from a polyhedral approximation , in: The Fifth International Conference on Computer Vision, 1995, pp. 902-907

[6] Evgeni Magid, Octavian Soldea, Ehud Rivlin. A comparison of Gaussian and mean curvature estimation methods on triangular meshes of range image data. Comput Vision and Image Understanding; 2007 ; 107: 139-159

[7] Kogure M., Akao Y., (1983),” Quality Function Deployment and Cwqc Japan” Qualità Progress, n.16, pp. 25-29.

[8] Apostol T. (1974). Mathematical Analysis. Addison-Wesley. pp. 344–345. ISBN 0-201-00288-4.

[9] Boissonnat JD. Geometric structures for three-dimensional shape representation. ACM Trans Graph 1984;3(4):266-86

[10] Jing Fu, Sanjay B.Joshi, Timothy W. Simpson. Shape differentiation of freeform surfaces using a similarity measure based on an integral of Gaussian curvature; Comput-Aided Des; 2008; 40: 311-323

[11] N. Dyn, K. Hormann, S.Kim, D.Levin, Optimizing 3d triangulation using discrete curvature analysis, in: T. Lyche, L.L. Schumaker (Eds.), Mathematical Methods in CAGD: Oslo 2000, Vanderbilt University Press, Nashville, TN, 2001, pp.135-146

[12] Desbrun M, Meyer M, Schroder P, Barr AH. Implicit fairing of irregular meshes using diffusion and curvature flow. In: Processings of the 26th annual conference on Computer graphics and interactive techniques. 1999. p. 317-24

[13] Erwin Kreyszig. Differential geometry. Toronto: University of Toronto press, 1959 –XIV. Mathematical exposition.

[14] L.Alboul, R. Van Damme, Polyhedral metrics in surface reconstruction: Tight triangulations, in : University of Twente, Department of Applied Mathematics, Technical Report, Memorandum No.1275 (1995) pp. 309-336

[15] S.J. Kim, C-H. Kim, D. Levin, Surface simplification using discrete curvature norm, in: The Third Israel-Korea Binational –conference on Geometric Modeling and Computer Graphics, Seoul, Korea, October 2001

[16] Guillaume Lavoué, Florent Dupont, Atilla Bakurt. A new CAD segmentation method, based on curvature tensor analysis;Comput-aided Des ; 2005; 37:975-987.

[17] Lavoue G, Dupon M, Baskurt A. Constant curvature region decomposition of 3D-meshes by a mixed approach vertex-triangle, J WSCG 2004, 12 (2) :245-52

[18] Cohen-Steiner D, Morvan J. Restricted Delaunay triangulations and normal cycle. 19th Annual ACM Symposium on Computational Geometri; 2003. P.237-46

[19] J.D. Foley, A. van Dam, S.K. Feiner and J.F. Huges. Computer graphics, principles and practice. Addison-Wesley, Reading, MA, second edition, 1992

[20] G.Golub and C.F. Van Loan. Matrix Computations. John Hopkins University Press, 1983

[21] Roland 3D Scanners http://www.rolanddg

[22] Barret O’Neill. Elementary differential geometry. Accademic press, New York and London, 1968